OPTICAL MODELLING OF VCSEL-ASSISTED THERMOPLASTIC TAPE PLACEMENT

T. Weiler[1], M. Emonts[1], P. Striet[1], S. Gronenborn[2] and H. Janssen[3]

[1] Aachen Center for integrative Lightweight Production AZL, RWTH Aachen, Steinbachstraße 19, 52074 Aachen, Germany

[2] Philips GmbH Photonics Aachen, Steinbachstraße 15, 52074 Aachen, Germany

[3] Fraunhofer Institute for Production Technology IPT, Fiber-Reinforced Plastics and Laser System Technology, Fraunhofer, Steinbachstraße 17, 52074 Aachen, Germany

Keywords: Automated, Thermoplastic, Tape, Placement, Vertical-Cavity Surface-Emitting Laser

Abstract

Due to high intensities and low response time, laser-assisted tape placement offers high processing speeds and precise temperature control. Therefore, the process and its systems gain more and more interest in several industries, which want to utilize continuously-reinforced thermoplastics. Especially high-volume production of structural and semi-structural components, like pressure vessels, pipes or automobile parts, is of interest. Further combinatorial potentials, like the combination with injection molding promise complex, yet cost-effective, product designs. Current laser-based tape placement systems are able to control the laser intensity distribution between tape and substrate by electro-mechanically tilting the laser optics or the whole laser beam source [1], [2]. The use of novel Vertical-Cavity Surface-Emitting Lasers (VCSEL) offers new possibilities to control the laser intensity distribution by use of discrete electrically-controllable emitter lines [3]. Tape and substrate can be heated independently with adjustable intensity profiles in the width or in feed direction. The basis for a *purposeful* laser intensity distribution is knowledge of the *intrinsic* process intensity distributions in the process zone, which depends on the process geometry, the VCSEL angular intensity distribution and the effect of laser reflection. This paper proposes a method to calculate the process intensity distribution for VCSEL-assisted tape placement.

1. Introduction

Mass customization requires the ability to manufacture a variety of parts with a limited number of highly-flexible machines and tools [4]. This is especially a challenge in the field of lightweight production, where manufacturing processes require a high degree of *reproducibility* and *control*, due to the *safety-critical* nature of the final products. Furthermore, a trend towards multi-material designs requires the processing of different fiber types and matrices, oftentimes in combination with metals.

In the case of thermoplastic tape placement, these trends lead to the specific challenge of heating varying pre-products and substrates with varying geometries and material attributes. Additional changing process conditions are already present in today's processes, like changing speeds, for example in start and stop procedures. These changing conditions, whether in-process or from-process-to-process, require an ability to locally adapt the laser intensity in the process zone. The use of novel Vertical-Cavity Surface-Emitting Lasers (VCSEL) offers new possibilities to control the laser intensity distribution by use of discrete electrically-controllable emitter lines. The basis for a *purposeful* laser intensity distribution is knowledge of the *intrinsic* irradiance distributions in the process zone, which depends on the process geometry and the VCSEL angular intensity distribution.

Excerpt from ISBN 978-3-00-053387-7

To analyze and describe the tape placement process holistically, GROUVE introduced a scheme on how to view the cause-and-effect chain, beginning from the beam source till the final structural attributes of the part [5]. The holistic scheme will in part be applied by AZL and Fraunhofer IPT for the general investigation and analysis of VCSEL-assisted tape placement, see **Figure 1**. For a full understanding of VCSEL-assisted tape placement, three major physical steps have to be considered: the *optical* process, the subsequent *thermal* process and the following *bonding* process. To identify the influencing variables in these three domains, three areas have to be considered: the material attributes, the system setup and the specific process condition. The following table summarizes the identified attributes, regarding the *optical process* of VCSEL-assisted tape placement:

Table 1. Attributes affecting the *optical process* of VCSEL-assisted tape placement.

Regarding	*Material attributes*	*System setup*	*Process condition*
Tape	- Absorption coefficient - Reflectance - Transmissivity	- VCSEL module angle - VCSEL module position - Power setting of emitters*2 - Wavelength - Beam intensity distribution - Roller geometry	- Angle of ray incidence - Irradiated area - Laser penetration depth - Velocity and Acceleration*1/ deceleration*1
Substrate	- Absorption coefficient*1 - Reflectance *1 - Transmissivity*1	- VCSEL module angle - VCSEL module position - Power setting of emitters*2 - Wavelength - Beam intensity distribution - Mold geometry	- Angle of ray incidence*1 - Irradiated area*1 - Laser penetration depth*1 - Velocity and Acceleration*1/ deceleration*1 - Substrate geometry*1

*1: not necessarily constant within process, *2: control variable

A further classification can be made by the question of whether these influencing variables can change within the process, or not. Several variables were identified and are marked with *1 in the table.

The focus of this paper lies on the first step of the cause-and-effect chain: the *process intensity distribution* $q'''(t)$ in the tape infeed area. The process intensity distribution is the basis to predict the temperature profiles, in the feed, width and thickness direction. It therefore represents an important aspect for the process design, especially if *in-situ consolidation* is pursued.

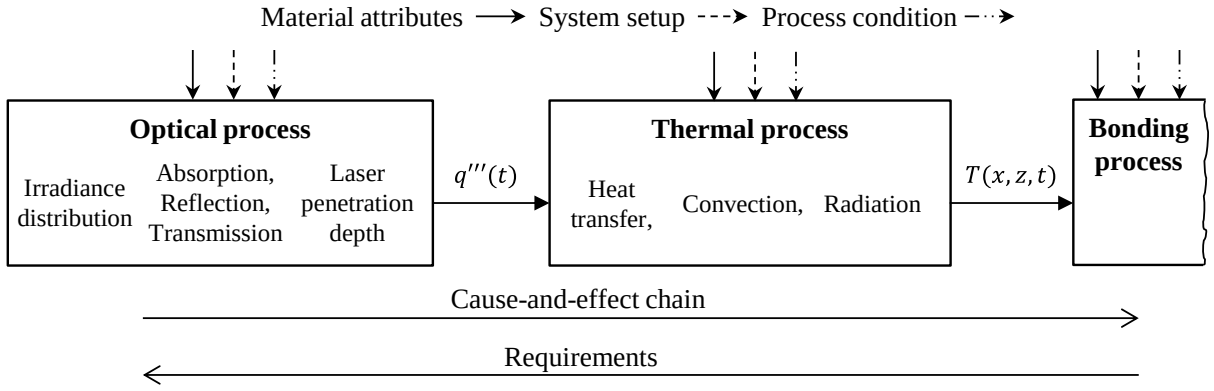

Figure 1: Cause-and-effect chain in tape placement, based on [4]

STROKES-GRIFFIN and GROUVE analyzed the optical process of diode-laser-assisted tape placement by means of *ray tracing* [5], [6], e.g. with a software like Zemax®. Both considered the effect of *reflectance*, which oftentimes can be neglected, especially when large areas of the process zone are irradiated with an *angle of irradiance* larger 60° [2], [8]. KOELZER has already considered the aspect of reduced irradiance in the shadowing area and a reduced irradiance, caused by the roller geometry in his thermal simulations [3]. This paper will propose a method to calculate the irradiance distribution for the case of VCSEL-assisted tape placement. The results will later be used by AZL and Fraunhofer IPT for thermal analysis of VCSEL-assisted tape placement processes.

Excerpt from ISBN 978-3-00-053387-7

2. Tape Placement by Use of Vertical-Cavity Surface-Emitting Laser

The Vertical-Cavity Surface-Emitting Laser (VCSEL) can be seen not as one single laser, but as many thousands of lasers, arranged in arrays of maximized packing density. By packing several thousand 30-µm-wide lasers densely, high overall intensities are achieved (see **Figure 2** and **Equation 1)**. 2205 single VCSELs are set on a wire-bonded chip. 56 of those chips are placed on a so called "emitter" and 28 of these chips are electrically connected in series and can be controlled independently by an electronic driver unit. (These 28 chips are placed in 2 rows of 14 chips each) [3].

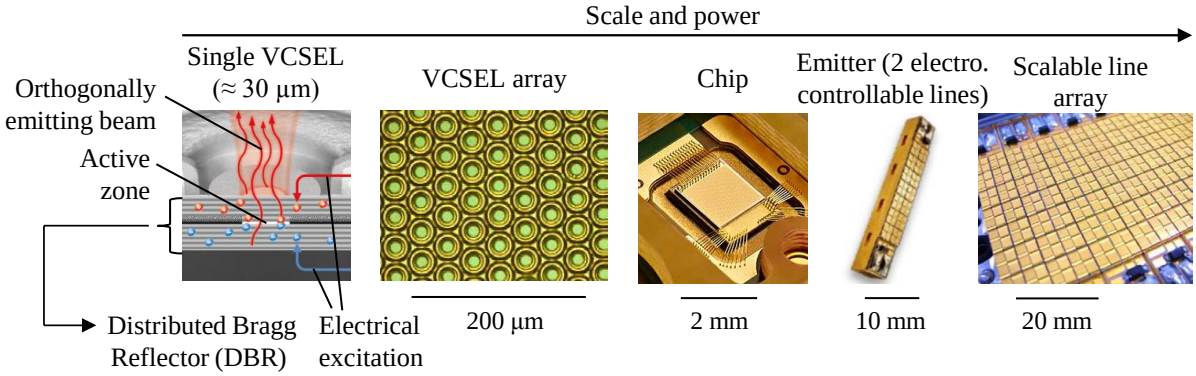

Figure 2: VCSEL technology from single micro laser up to scalable line arrays [Philips Photonics]

In combination with a cooling system, a power supply unit and a mechanical housing, these emitters are integrated into compact modules. These modules can be placed in the infeed area of a tape placement system (see **Figure 3**). It has to be pointed out that the modules can be *scaled infinitely wide* by integrating more and more emitter lines next to each other. The individual control of each emitter line enables a response time of *milliseconds* and enables a purposeful setting of irradiance profiles. (The benefits of these new possibilities will be addressed in later publications.)

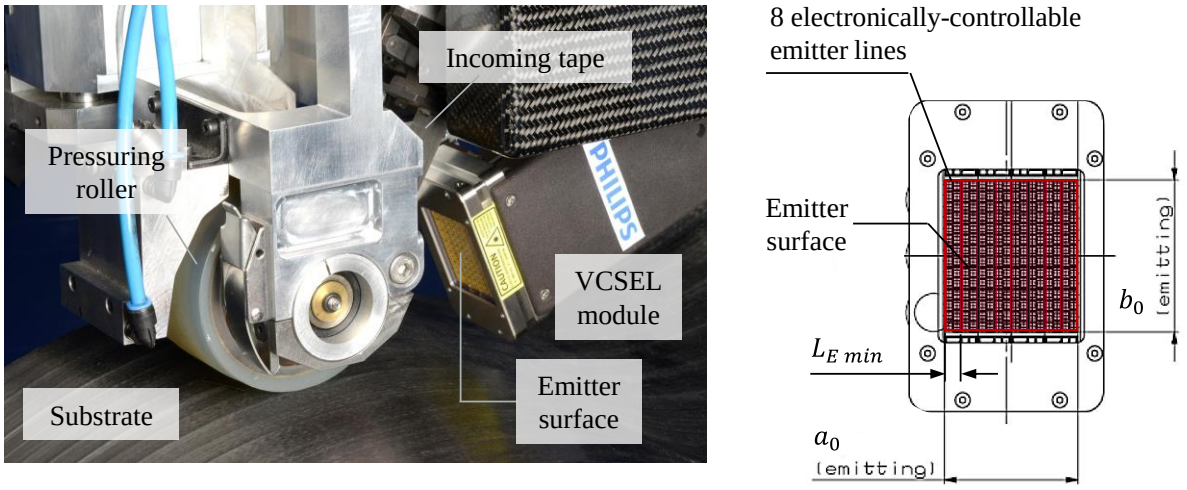

Figure 3: VCSEL-assisted tape placement system [Fraunhofer IPT]

The following **Table 3**, shows the different laser intensities, depending on the considered scale: single VCSEL (micro laser), single chip, emitter line and module. The difference between single VCSELs and chips emerge because of the area between the single VCSELs (compared **Figure 2**); the difference between the chips and the emitter lines emerges because of the space between the chips, which have to be connected to the emitter substrate by wire bonding. Further gaps between the emitters reduce the intensity slightly.

Excerpt from ISBN 978-3-00-053387-7

Table 3. VCSEL power characteristics, depending on the scale [Philips Photonics]

	Single VCSEL (micro laser)	*Chip*	*Controllable emitter line*	*Emitter (2 lines)*	*Module (line array)*
Consisting of:		2205 VCSLs	28 chips	56 chips	8 lines
Total power	0.0032 W	7.1 W	200 W	400 W	1600 W
Area	$\pi(0.005\ mm)^2$	1.8x1.7 mm²	40x4.3 mm²	40x8.6 mm²	40x34.3 mm²
Max. intensity in the near field	41 W/mm²	2.3 W/mm²	1.16 W/mm²	1.16 W/mm²	1.16 W/mm²

The *smallest controllable heating width* $L_{E\,min}$ of the VCSEL module (currently used by AZL and IPT) is defined by the width of the emitter lines: roughly 4.3 mm in the near field. This smallest controllable width increases with distance to the emitting surface, due to the divergence of each single VCSEL, compare **Figure 10**. The *maximum intensity* I_0 can be calculated easily by dividing the overall *optical power* of the module P_{module} with its *emitting surface* A_0 (**Equation 1**):

$$I_0 = \frac{P_{module}}{A_0} = \frac{1600\ W}{34.3\ mm \cdot 40\ mm} \approx 1.2 \frac{W}{mm^2} \tag{1}$$

The decrease of intensity can be estimated by considering the *distance to the emitting surface* d and the *global divergence angle* α of the laser beam, (which depends slightly on the laser power, more accurately: on the *electrical current* i):

$$I\big(d, \alpha(i)\big) = \frac{P_{module}}{A} = \frac{P_{module}}{(d \cdot tan\alpha + a_0) \cdot (d \cdot tan\alpha + b_0)} \tag{2}$$

In the far field, this approximation is not valid, because the more distant the considered area, the less radiation overlaps at the outer edges, compared to more overlaps in the center. It can be observed, that at a distance of 40 mm, the intensity is still 70 % of its maximum. Therefore it is in general beneficial to place a VCSEL module as near as possible relative to the material. Because most of the heating energy is induced in a region not far away from the system, see **Figure 13**, and because high processing speeds can be achieved, the effect of reduced intensity is not a significant issue, as it will explained later in the optical analysis in detail.

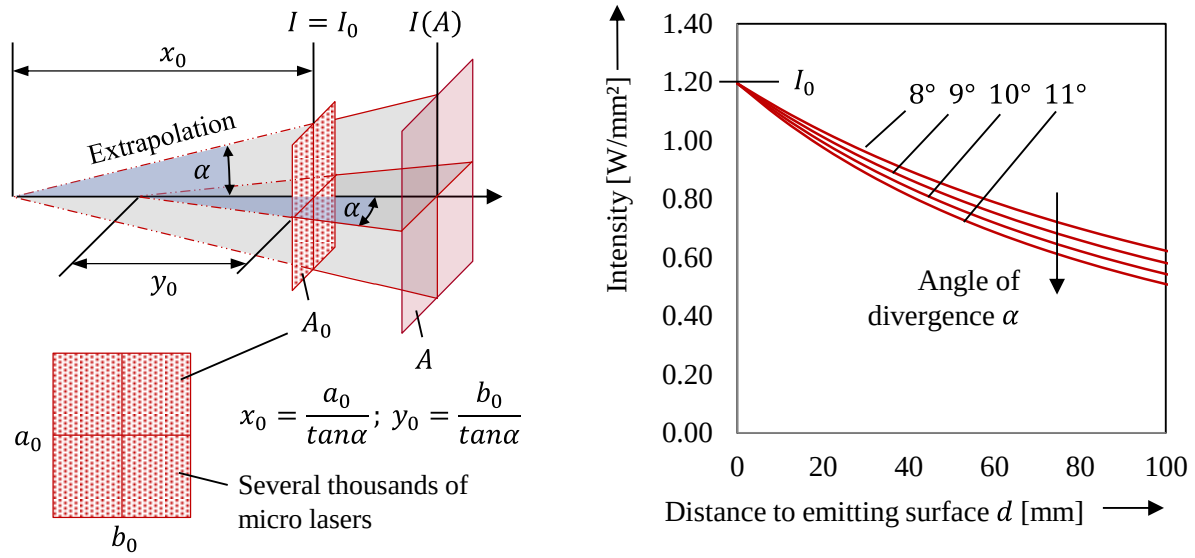

Figure 4: Approx. VCSEL intensity depending on distance to emitting surface and angle of divergence

Nonetheless, several alternative tape placement systems are feasible to reach a 100% use of the VCSEL radiation and are being developed by AZL and IPT in cooperation with Philips Photonics at the moment.

Excerpt from ISBN 978-3-00-053387-7

3. General Considerations

When laser radiation hits the surface of the material, the *power per area* on that surface will mostly be smaller than the general *laser intensity I*, due the *orientation* and *distance* of the object relative to the beam profile. This value will subsequently be called *irradiance E* with the same unit as the laser intensity *W/mm²*. If one takes a more closer look at the process zone of VCSEL-assisted tape placement, the general irradiance distribution in *material feed direction* can be described as follows: at first, the most outer single VCSELs begin to radiate on the tape with increasingly higher number, starting at P1 (see **Figure 5**), until a maximum is reached. From then on the irradiance on the material decreases, due to the divergence of the single VCSELs with a rate roughly described by **Equation 2**.

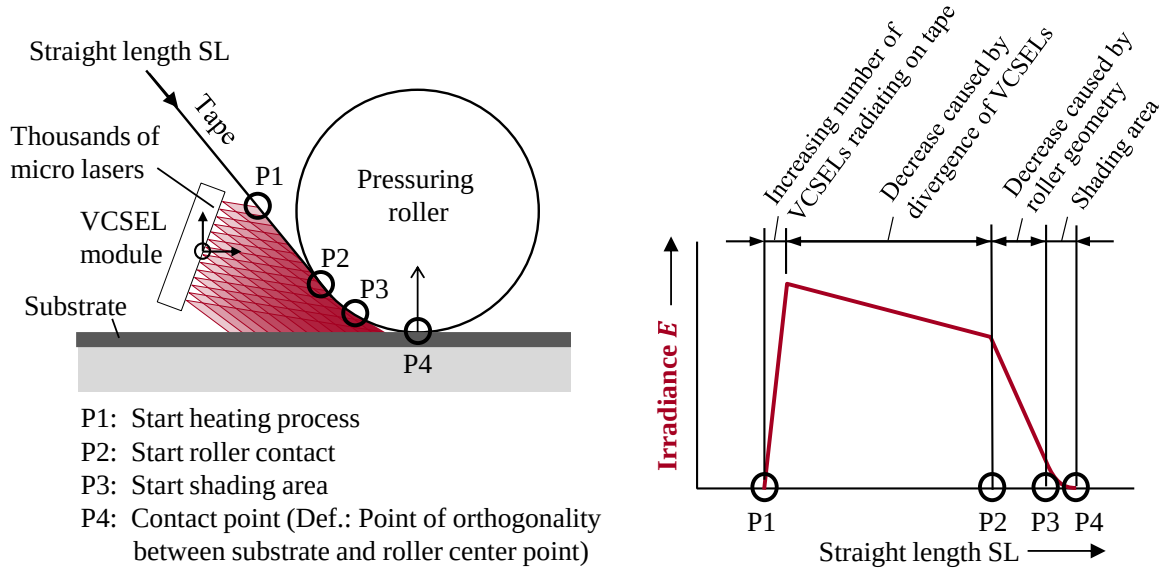

Figure 5: Generalized irradiance profile in VCSEL-assisted tape placement

When the tape contacts the roller (P2), the surface of the tape, which is being radiated on by the VCSEL rays, starts to increase, relative to the laser power in that area. This leads to a significant decrease of the irradiance and depends mostly on the *roller geometry*, see also **Figure 6**. This is not unique to VCSEL-assisted tape placement, but holds true for all laser-assisted tape placement processes. It also has to be pointed out that the *angle of incidence* also decreases in that area, which increases the effect of *reflectance*. At some point (P3) the VCSEL rays are not possible to reach the tape anymore (shading area). Further energy input can only happen now by forward-reflected rays.

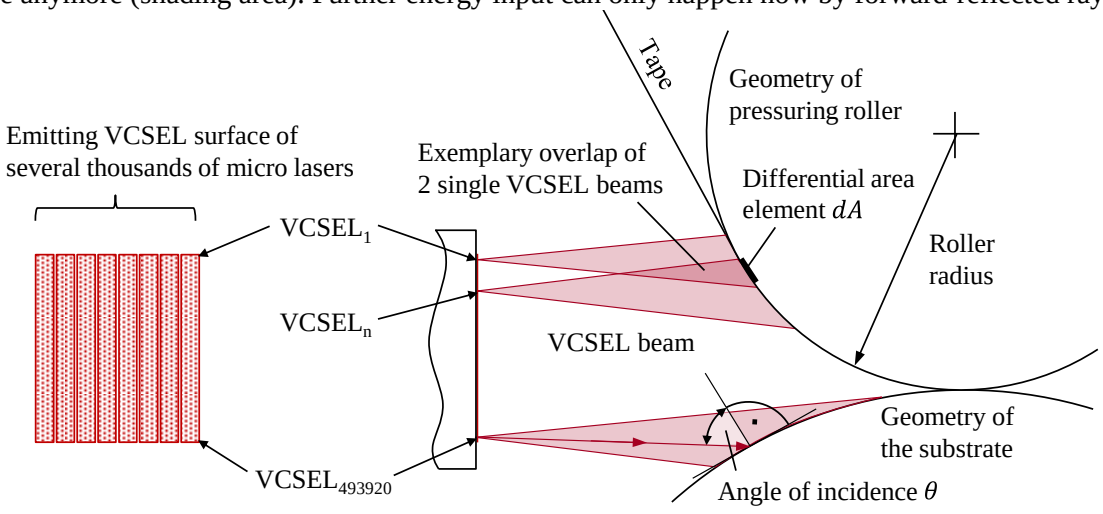

Figure 6: General process geometry with exemplary overlap of 2 VCSELs, which lead to the intrinsic irradiance distribution (*figure schematically drawn and not to scale*)

Excerpt from ISBN 978-3-00-053387-7

4. Optical Modelling

Optical effects and values in thermoplastic tape placement: A literature research has been done in order to determine possible optical effects and values of relevance for VCSEL-assisted tape placement (see **Figure 7**):

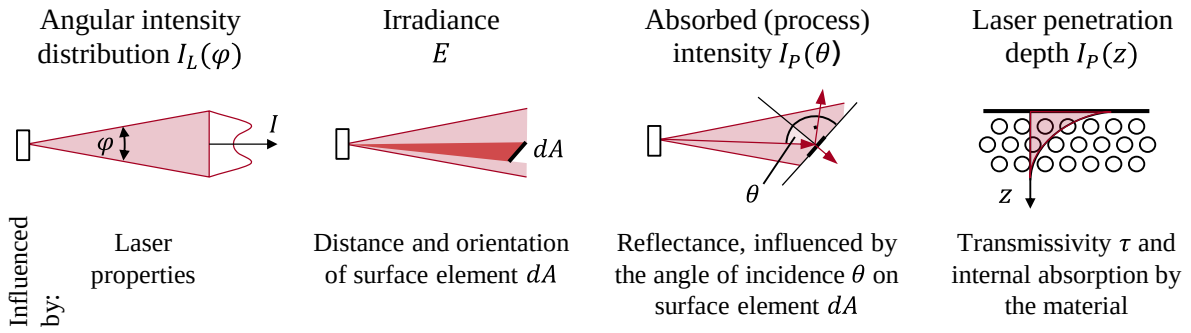

Figure 7: Optical effects and values in thermoplastic tape placement

The left three values will be considered in the analysis: the *angular intensity distribution* of the single VCSELs, the *irradiance on each surface element* in the process zone and the *absorbed intensity*, which depends on the effect of *reflectance*, due to the *angle of incidence* and material properties at the surface. The effect of the *laser penetration depth* will *not* be considered in this paper.

Solid angle: An important mathematical value for the analysis is the *solid angle* Ω with the unit *steradian* [sr]. The solid angle is the counterpart of the *conventional angle* of the unit *radiant* [rad]. Where the conventional angle describes the amount of spreading between two converging lines (full circle = 2π), the solid angle describes the amount of surface on a 3-dimensional sphere (full sphere = 4π). It simply adds 1 dimension to the conventional angle.

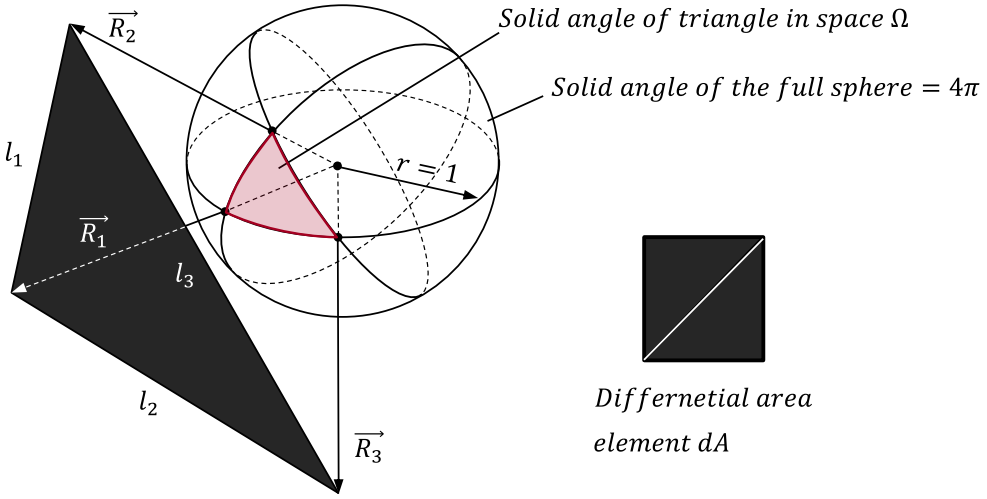

Figure 8: Calculation of the solid angle for a triangle in space [7]

It is possible to calculate the solid angle for the case of a *triangle in space* analytically, see **Figure 8**, as derived by OOSTEROM, see **Equation 3**.

$$\Omega = 2 \cdot \arctan\left(\frac{\mathrm{R}_1.(\mathrm{R}_2 \times \mathrm{R}_3)}{(\mathrm{R}_1 \cdot \mathrm{R}_2) \cdot \|\mathrm{R}_3\| + (\mathrm{R}_2 \cdot \mathrm{R}_3) \cdot \|\mathrm{R}_1\| + (\mathrm{R}_1 \cdot \mathrm{R}_3) \cdot \|\mathrm{R}_2\| + \|\mathrm{R}_1\| \cdot \|\mathrm{R}_2\| \cdot \|\mathrm{R}_3\|}\right) \quad (3)$$

Two triangles can be combined into a *quadrangular differential area element dA*, **Figure 6.** The derivation of the **Equation 3** is *not* part of this paper.

Excerpt from ISBN 978-3-00-053387-7

Measuring and modelling of VCSEL angular intensity distribution: For the exact calculation of the *irradiance distribution* each single VCSEL and the specific VCSEL angular intensity distribution was considered. The intensity of a single VCSEL is *rotationally symmetric* but *not homogeneous* and was therefore measured with a beam profiling camera (Ophir, L11059) in combination with an aspheric lens (AL5040-B - Ø50 mm S-LAH64, f = 40 mm, NA = 0.54, ARC: 650-1050 nm) [9]:

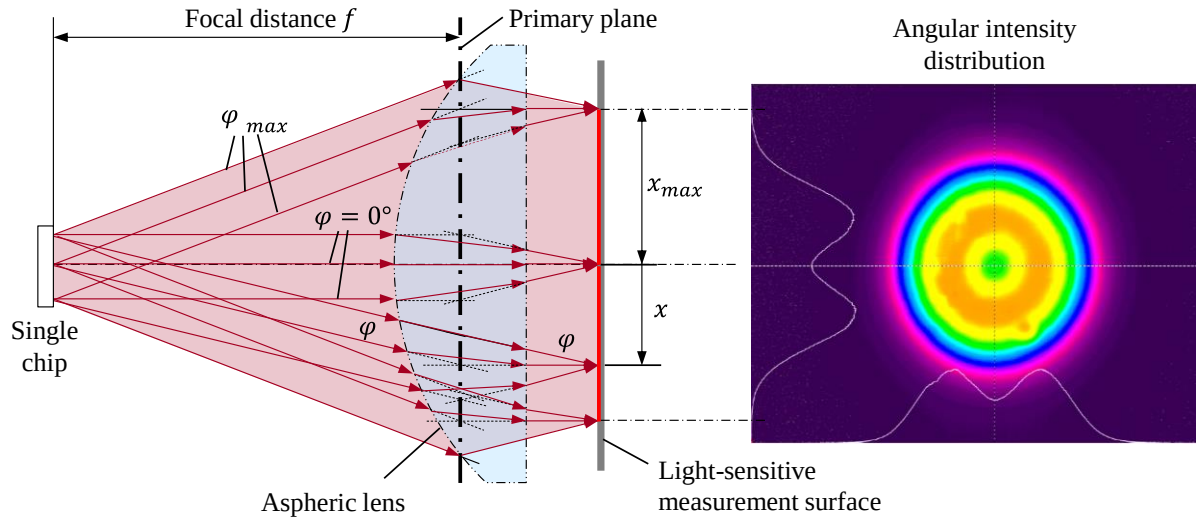

Figure 9: VCSEL beam angular intensity measurement (left) and result (right)

The aspheric lens diffracts all beam angles φ (of all VCSELs on the chip) to a certain radial distance x relative to the center on the measurement surface. The radial distance x on the measurement surface depends therefore on the beam angle φ in the form of:

$$\varphi = \arctan\left(\frac{x}{f}\right) \tag{4}$$

with f being the *focal distance* to the *primary plane* of the aspheric lens; in this case 40 mm. The measured data was modelled by curve fitting in Matlab®, see **Figure 10,** expressed in the form of **Equation 5**:

$$I_R(\varphi) = p_1 \cdot e^{-\left(\frac{\varphi}{p_2}\right)^2} + p_3 \cdot e^{-\left(\frac{\varphi}{p_4}\right)^2} \; [W/mm^2] \tag{5}$$

Because the aspherical lens *projects* the *spherical* intensity on the measurement surface without any distortion, the *intensity per area* can be transformed directly into the *intensity per solid angle*:

$$I_{sr}(\varphi) = I_R(\varphi) \cdot \frac{A_{sqhere}}{\Omega_{sphere}} = I_R(\varphi) \cdot \frac{4 \cdot \pi \cdot f^2}{4 \cdot \pi} = I_R(\varphi) \cdot f^2 \; [W/sr] \tag{6}$$

This transformation is useful for **Equation 7**. Finally, by dividing the measured intensity with the number of VCSELs on the measured chip (2205), the intensity profile of a single micro laser can be obtained:

Excerpt from ISBN 978-3-00-053387-7

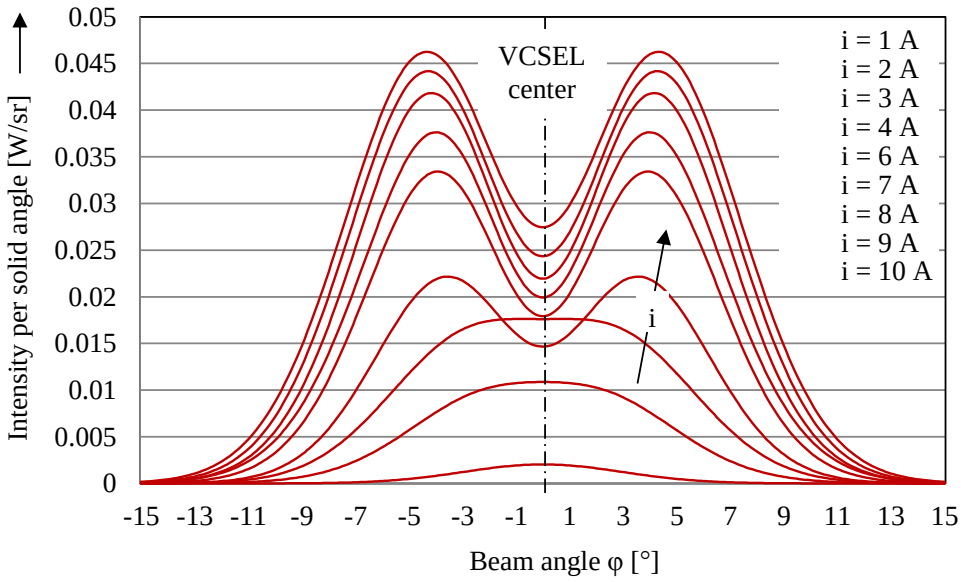

Figure 10: Modelled angular intensity distribution of single VCSEL

Furthermore, different VCSEL power settings lead to slightly different intensity profiles, see also **Figure 10.** The intensity per solid angle was therefore also measured at different *electrical currents* i.

Irradiance in the process by one VCSEL: The irradiance caused by one VCSEL on one differential area element in the process zone can now be calculated by the following **Equation 7**:

$$E_{dA}(\varphi, \Omega) = I_{sr}(\varphi) \cdot \frac{\Omega}{dA} \tag{7}$$

The irradiance depends basically on two geometrical attributes: the *angle* at which the element is irradiated by the VCSEL (compare **Figure 10** and see **Figure 6**) and by the solid angle of the element, which depends on the *orientation* and *distance* of the element relative to the VCSEL position.

Irradiance in the process by all VCSELs: The irradiance by all VCSELs on one differential area element $E_{dA\,i}$ in the tape placement processing zone can be calculated by the subsequent **Equation 8**.

$$E_{dA\,i} = \sum_{VCSEL_1}^{VCSEL_n} E_i(\Omega_i) \tag{8}$$

The equation states that the irradiance on one differential area element is the *sum* of all VCSELs radiating on that element, with consideration of the angular intensity distribution of each VCSEL (**Figure 6**). *Interference effects* can be ruled out, because the thousands of VCSEL "[…] emit incoherently and independently of each other."[3]

Irradiance in the process by all VCSEL on all elements: Finally, the calculation of **Equation 8** was applied to all differential surface elements of the tape placement process zone by an algorithm within the software Matlab®. The algorithm uses a geometrical model of the process zone to go through every differential area element and considers every VCSEL, which radiates on the elements. All intensities are summed up. The details of the algorithm are *not* part of this paper. **Figure 11** shows the result of the calculation. The result is one of two considered scenarios, which will be introduced in **chapter 4** (**Figure 13, left scenario**), in this case a tape *laying* scenario, without consideration of reflectance.

Excerpt from ISBN 978-3-00-053387-7

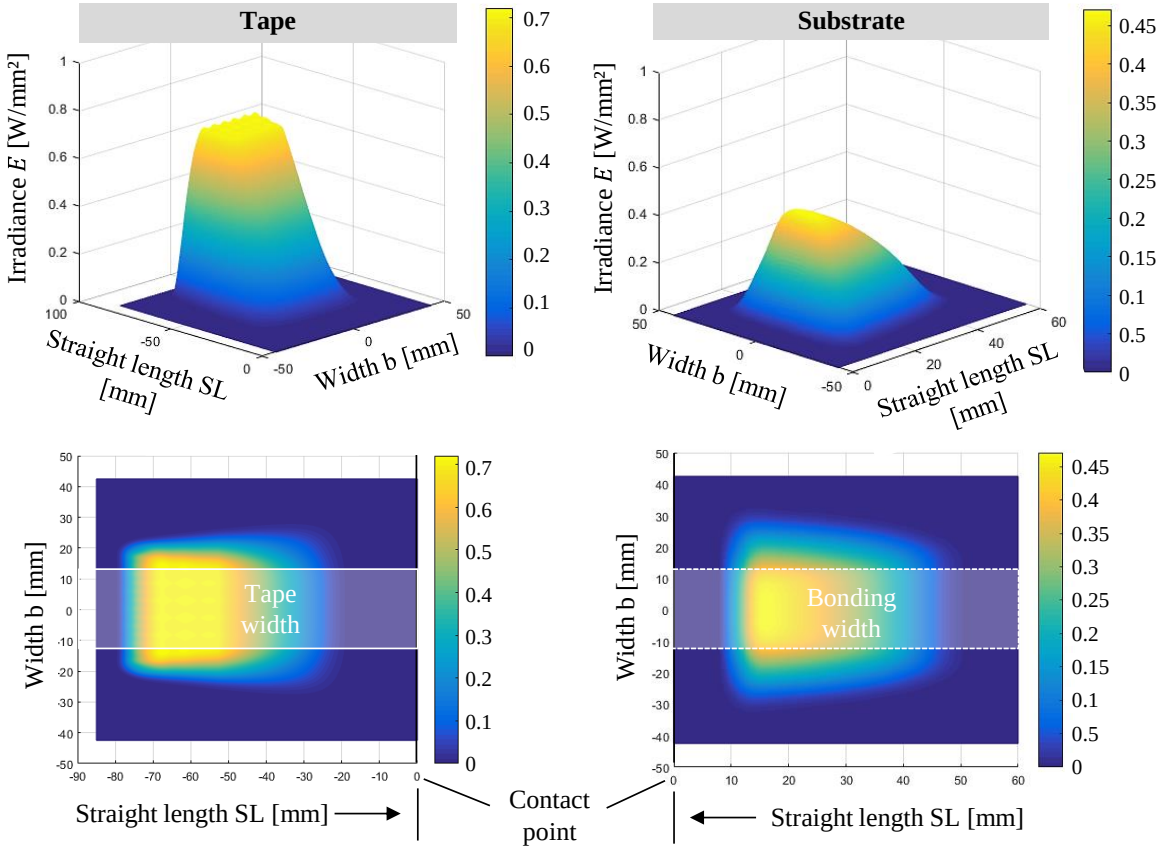

Figure 11: Principle result of the irradiance modelling for the tape (left) and substrate (right) for the exemplary case of tape *laying* from chapter 4

The *straight length SL* describes the distance to the *contact point* on the tape (see **Figure 5**). It is interesting to see that the irradiance decreases towards the contact point in the case of the tape (left picture), but increases in the case of the substrate (right picture). Furthermore, the irradiance profile on the tape is in general more narrow, probably because the VCSEL module is positioned more close to the tape, compared to the substrate, see again **Figure 13, left scenario (tape laying)**.

Effect of reflectance: Until now, the effect of reflectance was *not* considered. Some authors regard this effect as not significant in thermoplastic tape placement, e.g. STEYER [8], and set the absorption coefficient to 1. His assumption is that beams in the nip zone area reflect from tape and substrate respectively towards each other – no energy is lost. Others like STROKES-GRIFFIN investigate this process by ray tracing for the case of diode-laser-assisted tape placement [6].

The influence of reflectance for the case of VCSEL-assisted tape placement remains to be investigated. As the effect depends on the angle of incidence, which depends on the orientation of the process surface relative to the VCSEL module, it can never be fully ruled out that reflectance plays no role – it is specific for each tape placement scenario. We will analyze the effect for two exemplary cases of **chapter 4**, **Figure 13**.

In general, the *absorption*, the *reflectance* ρ and the *transmittance* τ depend upon each other:

$$1 = a + \rho + \tau \tag{9}$$

As the transmittance is in general very low in thermoplastic tapes, especially in carbon-fiber-reinforced tapes, it can oftentimes be neglected. Nonetheless, the *laser penetration depth* $I_P(z)$ may play a significant role for the heat flux distribution in the tape thickness, especially in non-blackened glass fiber tapes [10], but this effect will *not* be considered in this paper. Therefore, near surface absorption is assumed.

Excerpt from ISBN 978-3-00-053387-7

Model for the angular dependence of reflectance: First, a *quantitative measure* of the reflectance has to be known, which can depend on the angle of laser incidence. As tapes are intrinsically anisotropic (because of the unidirectional reinforcement), reflectance also depends on the *direction* of the laser incidence on the fibers [5]. Because most laser beams reach the surface in the fiber direction, we will only consider one direction for the analysis. STROKES-GRIFFIN modelled and measured the influence of beam angle on reflectance in [6]. It can be modelled mathematically by the following equation and will be used for our analysis:

$$\rho(\theta) = \rho_0 + 0.0002221 \cdot e^{0.09018 \cdot \theta} \tag{10}$$

For the case of transmittance being 0 follows that the absorption coefficient is:

$$a(\theta) = 1 - \rho(\theta) \tag{11}$$

For the analysis 0.1 will be used as the *base reflection coefficient* ρ_0 (respectively 0.9 as *base absorption coefficient* a_0), because the VCSEL wavelength is similar to the diode laser wavelength (980 nm), see [3], [2] and [8]. A significant decrease can be assumed for incidence angles >60°:

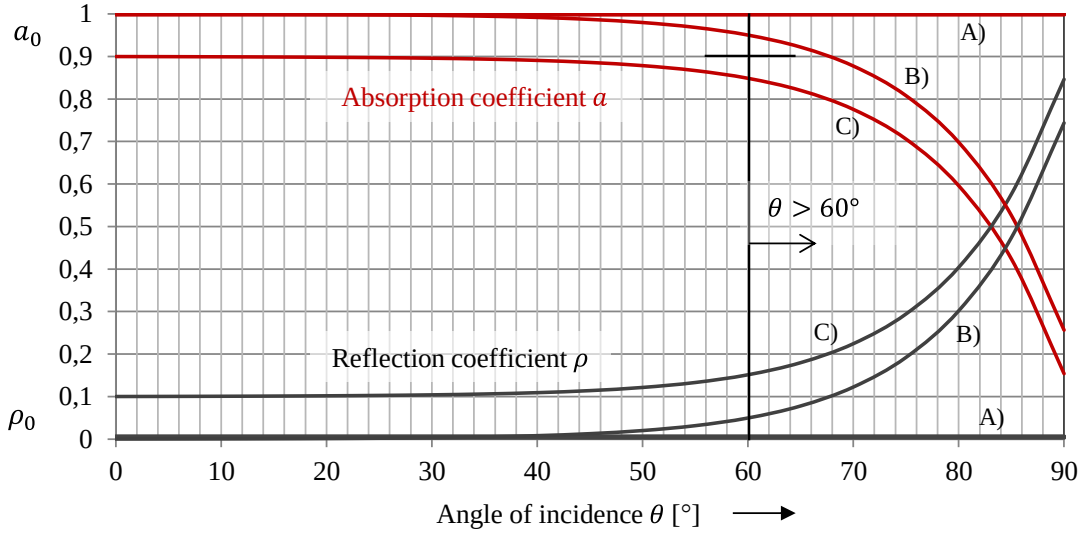

Figure 12: Angular dependence of reflectance and absorption as a function of incidence angle for carbon fiber PEEK tape, based on [6]

Whether reflectance plays a significant role depends on the specific orientation of each differential surface element in relation to the thousands of VCSELs, see again **Figure 6**.

Figure 14 and **Figure 15** show the principle result of the process intensity distribution; with and without consideration of reflectance:

A) Reflectance = 0, absorption = 1,

B) Reflectance = **Eq. 10**, with ρ_0 = 0; (a_0 = 1),

C) Reflectance = **Eq. 10**, with ρ_0 = 0.1; (a_0 = 0.9).

Results: For case C) the overall effect of reflectance on the *radiant exposure H* (see **Equation 12**) is roughly 16 %, both for tape and for substrate. Same applies also for case of tape *winding*. The effect of lower absorption at incidence angles >60° of **Equation 10** is relatively low: 6 %. The effect is therefore so low, because angles of >60° appear late in the process zone, at a place where much of the intensity of the laser has already been applied onto the material.

(It has to be pointed out, that the absorption coefficient can also slightly change at higher temperatures [2]. This effect is currently neglected. It would require knowledge of the thermal history already.)

Excerpt from ISBN 978-3-00-053387-7

4. Exemplary Analysis of Two VCSEL-Assisted Tape Placement Scenarios

Two exemplary tape placement scenarios were considered: tape *laying* on a flat mold and tape *winding* on a mandrel with the same radius as the pressuring roller – in this case 45 mm, see **Figure 13**. The *tape feed angle* was set to 67°; the VCSEL module to maximum power of 1600 W.

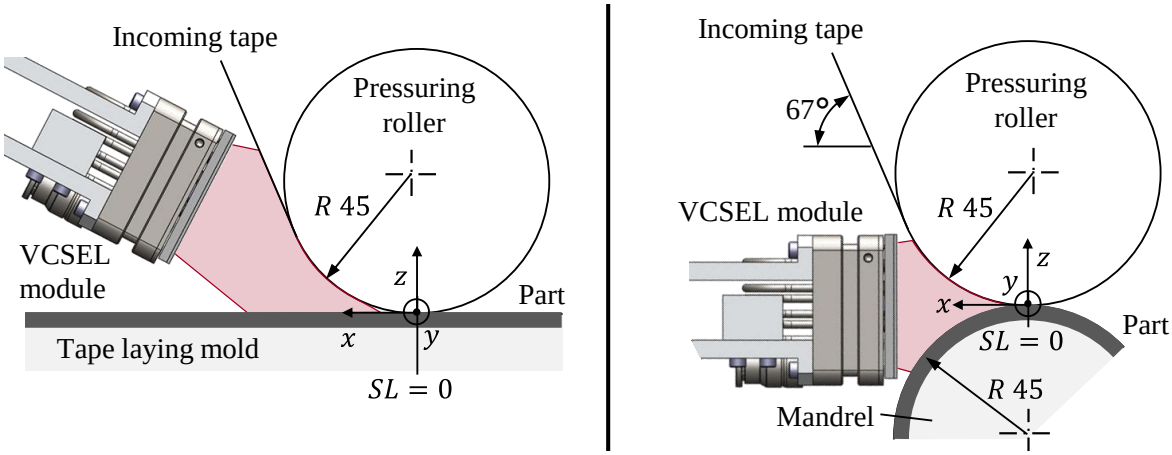

Figure 13: Cases for analysis. Left: tape laying, right: tape winding

In both cases, the VCSEL module was placed as near as possible to the tape with a distance ≥ 2 mm, with the purpose of reaching maximum irradiance and energy input. **Figure 14** and **Figure 15** show the *medium irradiance* over the width of the tape and the bonding zone (25 mm).

By integrating the medium irradiance over time, one can determine the *progression* and the *overall energy input* for the tape and the substrate, the *radiant exposure H*:

$$H = \int \bar{E}(t)dt \ [J/mm^2] \tag{12}$$

The integration requires knowledge of the tape placement *speed*, which can change over time. We assume a constant speed of 200 mm/sec. In the case of the tape most of the energy input is reached after 45 mm of heating (90 %). In this area the effect of reflectance is still low.

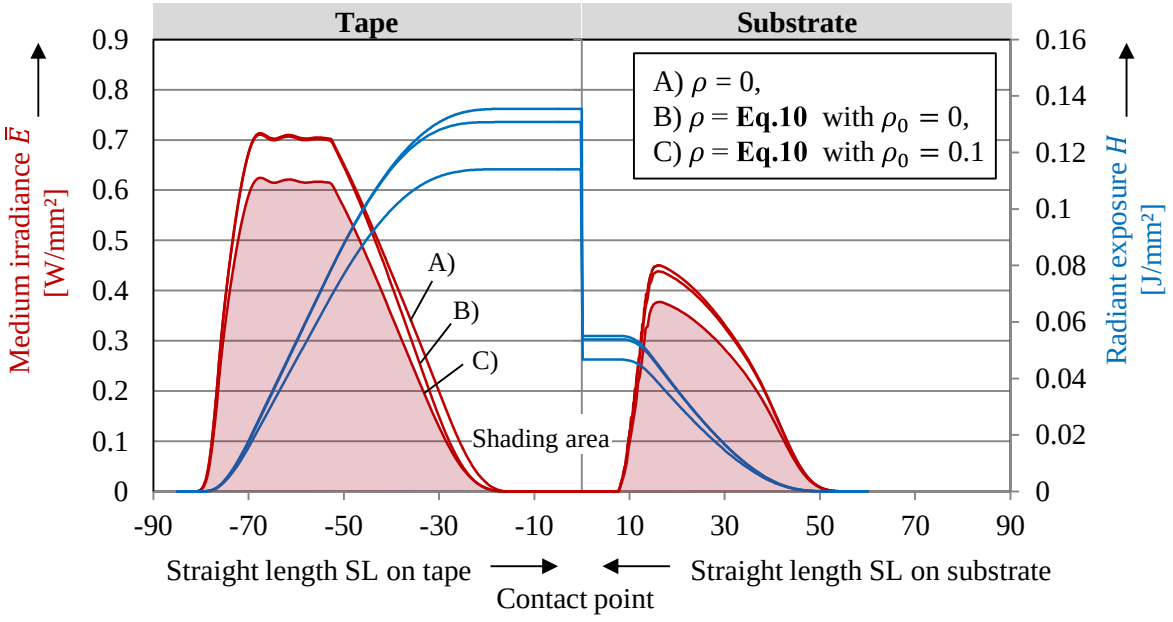

Figure 14: Process intensity distribution and radiant exposure for tape (left) and substrate (right) in the case of tape *laying*

Excerpt from ISBN 978-3-00-053387-7

It can also be observed that in the considered tape *laying* scenario, the radiant exposure between tape and substrate is quite *asymmetric*. A change of the *positioning* of the VCSEL module or an adaptation of the *intensity setting* of the emitters could be done accordingly.

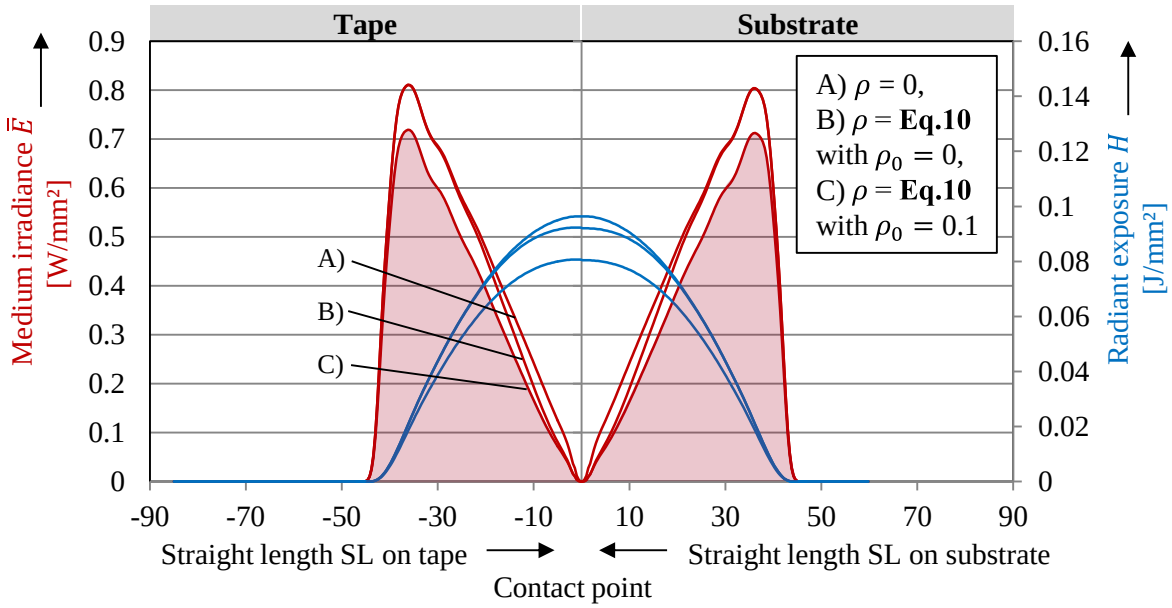

Figure 15: Process intensity distribution and radiant exposure for tape (left) and substrate (right) in the case of tape *winding*

The shading area in the considered tape winding scenario is quite small, because the VCSEL module was placed symmetrical and close to the pressuring roller and the mandrel – both have the same radius of 45 mm.

One can also derive from the analysis, that a change of the substrate geometry in a manufacturing process will naturally lead to (more or less) local changes in the process intensity – for example when asymmetric winding mandrels are used.

Finally, **Figure 16** presents a perspective view of the *(absorbed) process intensity distribution* in the nip area. Irradiance *and* reflectance are considered in these cases. The coordinate system lies again in the contact point (see **Figure 13**).

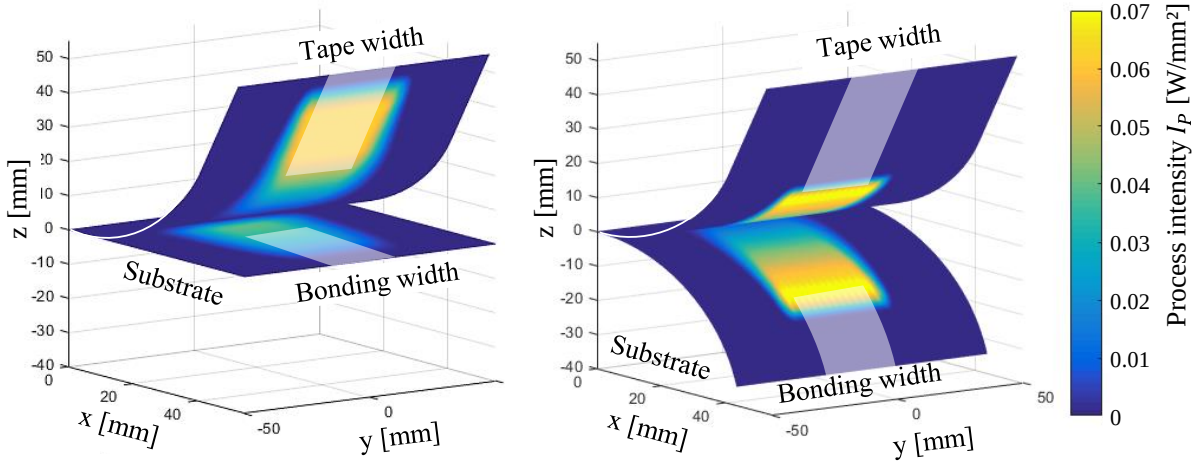

Figure 16: Isometric view of the (absorbed) process intensity distribution in the process for one case of tape laying (left) and one case of tape winding (right)

The acquired process intensity distributions can be used for thermal simulations in the future, see **Figure 1**.

Excerpt from ISBN 978-3-00-053387-7

5. Summary and Outlook

A method for the calculation of the *irradiance distribution* and the additional *influence of reflectance* in the process zone of VCSEL-assisted tape placement was presented. Two processing scenarios were analyzed: one for tape laying and one for tape winding. *Laser penetration depth* was *not* considered. This effect could further reduce the maximum intensity by a spreading of the laser light in the thickness of the tape. As a next step, the calculations will be validated by optical measurements of the overall beam profile of the VCSEL module and by short-time thermal imaging of the process zone. When the feasibility of the method can be validated it will be used for a thermal analysis of VCSEL-assisted tape placement processes in the near future.

Acknowledgments

The authors wish to thank the German Federal Ministry of Education and Research (BMBF) for the financial support granted to conduct this study within the Aachen Research Campus Digital Photonic Production (DPP), sub-project: Nano Digital Photonic Production (Nano-DPP), grant number 13N13476. Special thanks are due to the students supporting the research, colleagues of Fraunhofer IPT, Aachen Center for integrative Lightweight Production (AZL), Philips Photonics and the Chair for Technology of Optical Systems (TOS) for the valuable discussions and inspiring cooperation, which led to the content of this paper.

References

[1] Brecher C.; Emonts M.; Werner D.: Multi-Material-Head – Modulares und laserunterstütztes Tapelegesystem. Lightweight Design 04/2014, Produktions- und Fertigungstechnik, p.50-55.
[2] Koelzer P.: Temperaturerfassungssystem und Prozessregelung des laserunterstutzten Wickelns und Tapelegens von endlos faserverstärkten thermoplastischen Verbundkunststoffen. PhD Thesis, RWTH Aachen, 2008.
[3] Moench H.; Conrads R.; Deppe C.; Derra G.; Gronenborn S.; Gu X.; Heusler G.; Kolb J.;, Miller M.; Pekarski P.; Pollmann-Retsch J.; Pruijmboom A. Weichmann U.: High power VCSEL systems and applications. Proceeding of SPIE Vol. 9348, 93480W, 2015.
[4] Kull H.: Mass Customization – Opportunities, Methods, and Challenges for Manufacturing. Springer-Verlag Berlin and Heidelberg. 2015.
[5] Grouve W.: Weld strength of laser-assisted tape-placed thermoplastic composites. PhD Thesis, University of Twente, Enschede, the Netherlands, 2012.
[6] C.M. Stokes-Griffin; P. Compston: A combined optical-thermal model for near-infrared laser heating of thermoplastic composites in an automated tape placement process. Composites: Part A. Elsevier. 2014.
[7] Van Oosterom A.; Strackee J.: The Solid Angle of a Plane Triangle. IEEE Transaction on Biomedical Engineering, VOL. BME-30, NO. 2, 1983.
[8] Steyer M.: Laserunterstütztes Tapelegeverfahren zur Fertigung endlosfaserverstärkter Thermoplastlaminate. PhD Thesis. RWTH Aachen. 2013.
[9] Gronenborn S., Philips Photonics, private communication
[10] Stimpfl J.: CO_2-laserunterstütztes Tapelege-/Wickelverfahren zur Verarbeitung von ungefärbten, endlos glasfaserverstärkten Thermoplast-Tapes. PhD Thesis, RWTH Aachen 2015.

Excerpt from ISBN 978-3-00-053387-7